INTER-NOISE 2006

3-6 DECEMBER 2006
HONOLULU, HAWAII, USA

Finite element development of honeycomb panel configurations with improved transmission loss

Ferdinand W. Grosveld[a]
Lockheed Martin Engineering and Sciences
Mail Stop 463
NASA Langley Research Center
Hampton, VA 23681
USA

Daniel L. Palumbo[b], Jacob Klos[c]
and William D. Castle[d]
NASA Langley Research Center
Mail Stop 463
Hampton, VA 23681
USA

ABSTRACT

The higher stiffness-to-mass ratio of a honeycomb panel compared to a homogeneous panel results in a lower acoustic critical frequency. Above the critical frequency the panel flexural wave speed is acoustically fast and the structure becomes a more efficient radiator with associated lower sound transmission loss. Finite element models of honeycomb sandwich structures are presented featuring areas where the core is removed from the radiating face sheet disrupting the supersonic flexural and shear wave speeds that exist in the baseline honeycomb panel. These modified honeycomb panel structures exhibit improved transmission loss for a pre-defined diffuse field sound excitation. The models were validated by the sound transmission loss of honeycomb panels measured in the Structural Acoustic Loads and Transmission (SALT) facility at the NASA Langley Research Center. A honeycomb core panel configuration is presented exhibiting a transmission loss improvement of 3-11 dB compared to a honeycomb baseline panel over a frequency range from 170 Hz to 1000 Hz. The improved transmission loss panel configuration had a 5.1% increase in mass over the baseline honeycomb panel, and approximately twice the deflection when excited by a static force.

1   INTRODUCTION

Honeycomb core sandwich panels have widespread use in the aerospace industry as aircraft floor or wall panels. The higher stiffness-to-mass ratio of a honeycomb panel compared to a homogeneous panel results in a lower acoustic critical frequency. At the critical frequency a resonance occurs when the acoustic wavelength of the radiated sound wave propagating parallel to the panel surface matches the structural flexural wavelength. Above the critical frequency resonances occur at different angles of sound incidence as the sound trace wavelength equals the structural bending wavelength. The flexural wave speed is called acoustically fast or supersonic above the critical frequency. The structure becomes a very efficient radiator resulting in a lower sound transmission loss than exhibited by a homogeneous panel of the same mass.[1] Researchers have attempted to improve the transmission loss performance by optimizing the mechanical properties of the panels or by increasing the structural damping.[2-4] Modal distribution,[5,6] dynamic properties,[7-9] and acoustic characteristics[9] of honeycomb panels have been investigated to obtain a better understanding of the vibro-acoustic response of these sandwich structures. The wavenumber frequency spectrum has been employed to illustrate the dispersion behavior of a panel below and above the critical frequency.[11-13] The numerical modeling of the honeycomb panel vibratory behavior has been reported in numerous publications, some of which[14-17] are listed in the References section. Non-resonant and resonant transmission loss of sandwich

[a] Email address: f.w.grosveld@larc.nasa.gov
[b] Email address: daniel.l.palumbo@nasa.gov
[c] Email address: jacob.klos-1@nasa.gov
[d] Email address: william.d.castle@nasa.gov

structures were computed in Reference 15 with the use of dispersion curves, panel radiation efficiency and panel modal density. Recently, structural-acoustic finite element and boundary element models have been developed at the NASA Langley Research Center to describe and predict the sound radiation from and the transmission loss of honeycomb type structures.[18-23] In this paper finite element models are presented of honeycomb sandwich structures featuring areas where the core is removed from the radiating face sheet disrupting the supersonic flexural and shear wave speeds that exists in the baseline panel. These honeycomb panel structures exhibit improved transmission loss for a pre-defined diffuse sound field excitation. The panel energy dissipation was assumed small compared to the transmitted sound. The models were verified with the results from transmission loss measurements conducted in the Structural Acoustic Loads and Transmission[24] (SALT) facility at the NASA Langley Research Center. The frequency band of interest extended from 100 to 1000 Hz (5 Hz bandwidth). The upper frequency was limited by the computer execution time of the finite element analysis while the lowest frequency was determined by the ability to produce a diffuse sound field in the SALT reverberation chamber.

2   WAVENUMBER ANALYSIS

The baseline honeycomb panel had a square sound exposed area of 1.365 m^2 and an edge length of 1.168 m. A 19.05 mm thick Nomex core was sandwiched between two 0.508 mm thick aluminum face sheets, similar to honeycomb panels found in aircraft applications.[3] Selected material properties of the aluminum face sheets and the Nomex core are listed in Table 1.

Table 1. Selected material properties for the aluminum honeycomb face sheet and the Nomex core.

Aluminum face sheet			Nomex honeycomb core		
t	[mm]	0.508	t	[mm]	19.05
E	[N/m^2]	7.1 +10	G_{cx}	[N/m^2]	4.482 +7
			G_{cy}	[N/m^2]	2.344 +7
ρ_f	[kg/m^3]	2700	ρ_c	[kg/m^3]	48.06
c_L	[m/s]	5432	c_{Sx}	[m/s]	965.8
			c_{Sy}	[m/s]	698.4

The compressional wave speed in the face sheet material is given by[25]

$$c_L = \left[\frac{E}{\rho_f (1 - v^2)} \right]^{1/2}$$

where E is the Young's modulus, ρ_f is the density, and v is the Poisson's ratio. The speed of the shear waves in the core material are defined by[25]

$$c_S = \left[\frac{G_c}{\rho_c} \right]^{1/2}$$

where G_c is the shear modulus and ρ_c is the density. The shear modulus is different in the ribbon and the transverse directions of the honeycomb core (Table 1). At low frequencies the honeycomb is dominated by bending of the entire structure while at high frequencies, outside the frequency range of interest, the response is mostly controlled by the bending characteristics of the face sheets. Transverse shear in the honeycomb core governs the behavior in the mid-frequency region. A sixth order polynomial is given in Reference 2 describing the propagation speed of transverse waves as function of frequency. Defining the wavenumber as the ratio of the rotational frequency ω and the characteristic speed, this relationship can be expressed as

$$k_h^4 k_f^4 + k_s^2 k^2 k_f^4 - k^4 k_f^4 - k_s^2 k^6 = 0$$

where k_h is the bending wavenumber of the honeycomb sandwich, k_f is the bending wavenumber of a single face sheet loaded with half the mass of the core layer, k_s is the shear wavenumber for the core layer loaded with the mass of the face sheets and k is the wavenumber in air. Expressing the wavenumbers in terms of their material wave speeds and correcting for the additional mass loading yields the following expressions for k_h, k_s and k_f

$$k_h = \left[\frac{2(\rho_c t_c + 2\rho_f t)}{\rho_f t t_c (2t + t_c)} \frac{\omega^2}{c_L^2} \right]^{1/4} ; \quad k_s = \left[\frac{\rho_c t_c + 2\rho_f t}{\rho_c t_c c_S^2} \right]^{1/2} ; \quad k_f = \left[\frac{6(\rho_c t_c + 2\rho_f t)}{\rho_f t^3} \frac{\omega^2}{c_L^2} \right]^{1/4}$$

where t is the face sheet thickness and t_c is the thickness of the honeycomb core. The wavenumbers as function of frequency are shown in the dispersion plot of Figure 1. The speed of sound in air is constant with frequency and the wavenumber is shown as a straight line. The bending wavenumber curve of the honeycomb sandwich crosses the air wavenumber line at the critical frequency. The critical frequency was calculated to occur at 414 Hz. Resonances take place at the coincidence frequencies for different angles of the acoustic incident wave. Above the critical frequency the structural waves are acoustically fast (supersonic) and the panel acoustic radiation is much more efficient than for a panel radiating at frequencies below the critical frequency (subsonic). The shear wavenumbers for the core are indicated in Figure 1 by the short
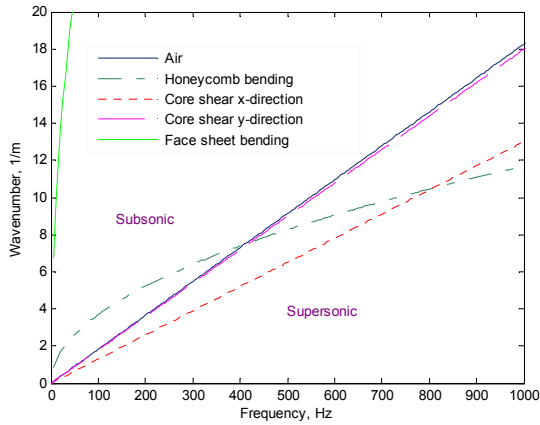

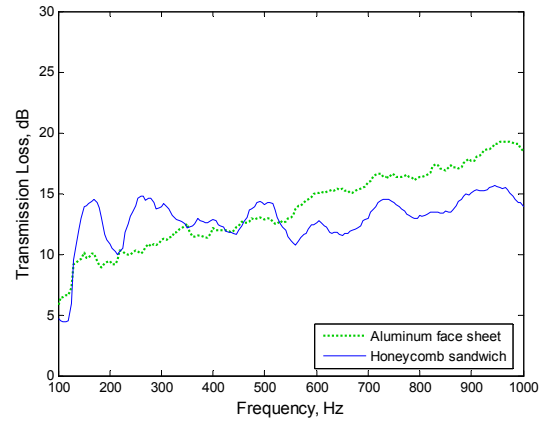Figure 1. Dispersion plot of characteristic wavenumbers as function of frequency.

Figure 2. Measured sound transmission loss of the honeycomb panel (3.66 kg/m^2) and an aluminum panel with the same thickness as the face sheet (1.37 kg/m^2).

dashed and long dashed lines for two perpendicular directions. The lower shear stiffness boasts the lower radiation efficiency. The shearing behavior is non-dispersive and is constant with the frequency. The bending of the honeycomb sandwich will gradually transform to a dynamic response dominated by the shearing of the core over a frequency region delineated by the frequencies at which each of the core shear wavenumber lines cross the wavenumber curve for the honeycomb sandwich. These frequencies were calculated to occur at 427 Hz and 817 Hz. It is shown in Figure 1 that the waves dominated by the core shear are acoustically fast and therefore radiate more efficiently than the acoustically slow waves. The wavenumber curve for a single aluminum face sheet by itself is shown on the left side in Figure 1. The bending waves in the face sheet are acoustically slow and radiate sound less efficiently than the acoustically fast waves, which results in higher transmission loss. This is illustrated in Figure 2 where the

measured transmission loss of the honeycomb sandwich panel is compared with the measured transmission loss of an aluminum panel with the same thickness as one of the face sheets. The transmission loss of the aluminum face sheet is indicated by the green dotted line and increases from about 13 dB at 500 Hz to about 19 dB at 1000 Hz, consistent with the classic mass law. However, the average transmission loss of the honeycomb sandwich panel stays nearly unchanged over the same frequency range. Above 500 Hz the transmission loss of the aluminum panel, with a surface mass of 1.37 kg/m^2, is even greater than the transmission loss of the honeycomb sandwich, which has a surface mass almost three times as high (3.66 kg/m^2). To improve the transmission loss of the honeycomb panel the stiffness to mass ratio could be lowered, which would result in a higher critical frequency and would broaden the frequency range of acoustically slow wavenumbers. Another option would be to lower the shear stiffness in the core until both shear waves in Figure 1 would be radiating acoustically slow. In this paper areas of acoustically slow wave speeds are created on the radiating panel surface to improve the sound transmission loss. This is accomplished by removing all or part of the honeycomb core thickness from the radiating face sheet in those areas. These configurations are referred to as voided core (the entire core removed) or recessed core (part of the core thickness removed) honeycomb panels. A sketch of a rectangular voided core honeycomb panel is depicted in Figure 3 showing the acoustically excited (exterior) face sheet, the voided honeycomb core and the radiating (interior) face sheet with the areas of subsonic wave speeds.
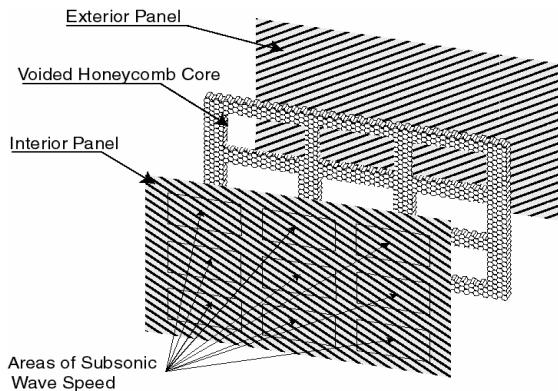

Figure 3. Sketch of a rectangular honeycomb panel with a voided core, creating areas of subsonic wave speed for improved transmission loss.
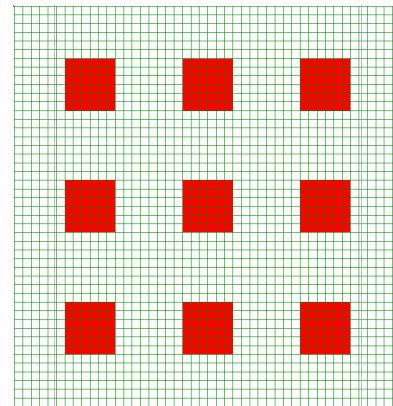

Figure 4. Sketch of the honeycomb panel featuring nine 152 mm square voids in the core.

3   FINITE ELEMENT HONEYCOMB PANEL CONFIGURATIONS

Four finite element honeycomb panel configurations were modeled and analyzed to predict the sound transmission loss characteristics. The first honeycomb finite element model featured nine 152 mm square voids in the core (Voided 9-152) as shown in Figure 4. The voids were arranged with a 203 mm separation. The second configuration (Figure 5) shows a honeycomb finite element model with nine 254 mm square voids in the core (Voided 9-254). The separation between these voided areas was 102 mm. While the finite element models were analyzed, test panels were manufactured for verification of the predicted transmission loss. A picture of the Voided 9-254 honeycomb test panel, just before final assembly, is shown in Figure 6. The face sheet in the foreground has the voided honeycomb core attached. The other face sheet has (green) glue applied around and between the voids. The voids in the core obviously weaken the honeycomb panel. The third finite element model was therefore designed to retrieve some of the lost rigidity by leaving 6.35 mm of the core material attached to the exterior face sheet in the

nine 254 mm square areas (Figure 7). The recessed core was covered by a 0.41 mm thick aluminum patch creating a 7.27 mm thick (including the thicknesses of the face sheet and the patch) honeycomb sub panel. This third configuration was designated Recessed 9-254. Finally, the fourth finite element model (Recessed 25-152) had twenty-five 152 mm square recessed core areas separated by only 25.4 mm, adding more strength to the honeycomb sandwich. The total recessed core area for the Recessed 25-152 and the Recessed 9-254 panels was about the same.
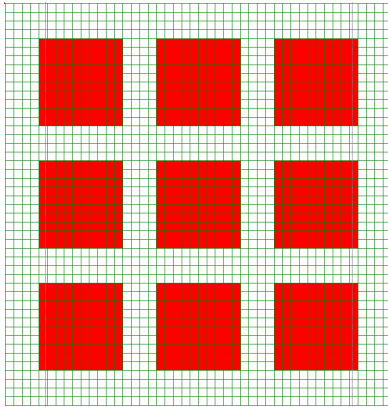

Figure5. Sketch of the honeycomb panel featuring nine 254 mm square voids in the core.

Figure 6. The voided honeycomb panel before final assembly showing one face sheet with nine 254 mm voids in the core and one face sheet partially covered with glue.
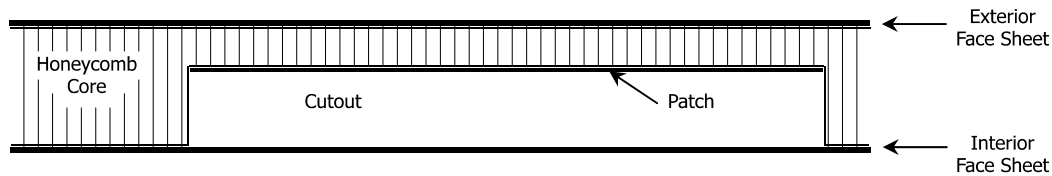

Figure 7. Cross-section of the honeycomb panel with the 6.35 mm recessed core and a 0.41 mm aluminum patch.

The geometrical parameters of the four configurations are summarized in Table 2.

Table 2. Characteristic geometries of the honeycomb finite element models.

Honeycomb configuration	Number cutouts	Core thickness [mm]	Cutout length and width [mm]	Cutout area [m^2]	Total cutout area [m^2]	Patch
Base panel	none	19.05	N/A	N/A	N/A	N/A
Voided 9-152	9	0.0	152	0.023	0.208	No
Voided 9-254	9	0.0	254	0.065	0.581	No
Recessed 9-254	9	6.35	254	0.065	0.581	Yes
Recessed 25-152	25	6.35	152	0.23	0.578	Yes

4   FINITE ELEMENT ANALYSIS

The honeycomb panel finite element models were developed using the pre/post processor MSC/Patran[®] and were analyzed in MSC/Nastran.[®] Each of the two honeycomb face sheets was modeled with 2,116 CQUAD4 plate elements while the core consisted of 2,116 CHEX8 solid elements with three-dimensional anisotropic material properties. The honeycomb panel was mounted in a stiffened steel frame window in the SALT facility. The steel frame was also included in the finite element models and consisted of CHEX8 solid elements. The dimensions of the elements for the face sheets were 25.4 mm squared and were chosen to be small compared

to the acoustic wavelength at 1000 Hz. A diffuse acoustic excitation for the finite element models was developed based on plane wave propagation.[22] A large number (1000) of plane waves having random angles of incidence, random magnitudes, and random temporal phase angles were summed to simulate a diffuse field excitation. The pressure acting on the surface of each element in the finite element model, due to N plane waves, was computed using the coordinates of the element centroids. The pressure distribution acting on each of the 2,116 surface elements was used as the acoustic excitation and was assumed to be uniformly distributed over each element. The incident sound power was computed from the intensity vector of each of the N plane waves. The intensity vector of the nth plane wave is given as

$$\bar{I}_n = -\frac{[P_n \cos(\theta_n)]^2}{\rho c}[\sin(\theta_n)\cos(\psi_n)\bar{i} + \sin(\theta_n)\sin(\psi_n)\bar{j} + \cos(\theta_n)\bar{k}]$$

where P_n is the steady state pressure of a single plane wave, and θ_n and ψ_n are the tilt and azimuth angles of incidence. The intensity normal to the surface of each element of the finite element model is found from the dot product of the intensity vector and the element normal $\bar{r}_e$. The total sound power incident on the panel with surface area A_E can be calculated for all N plane waves and E elements from

$$\Pi_i = \sum_{e=1}^{E}\sum_{n=1}^{N} A_e \bar{I}_n \cdot \bar{r}_e$$

Frequency response functions were computed for excitation by ten sets of the random incidence sound fields. Velocity distributions over the panel surface were output in finite element punch files for post processing. The radiated acoustic power was computed from the finite element calculated velocity distribution over the panel, using the radiation resistance matrix $(\Re)$ approach.[26] In this approach the total acoustic power is obtained from the unique contributions of an array of elemental radiators on the surface of a baffled structure. The elements are much smaller than the acoustic wavelength. The diagonal elements of the radiation resistance matrix equal unity while the remainder of the symmetric matrix is populated with the terms $sin(kr_{ij})/kr_{ij}$. The parameters r_{ij} represent the distances between each finite element i and each finite element j. All matrix elements are then multiplied by $\omega^2\rho A_e^2/(4\pi c)$ to obtain $\Re$. The radiated acoustic power is obtained from

$$\Pi_r = v_m^H \Re v_m$$

where v_m is the velocity matrix containing the frequency response calculated velocity for each finite element and v_m^H is the conjugate transpose of the velocity matrix. The radiation matrix[26] was derived for a panel with simply supported edges in an infinite baffle. The honeycomb panel is assumed to have simply supported edge conditions. However, the areas where the core was removed from the aluminum face sheet will not always follow the modal behavior of the honeycomb sandwich panel but instead have their own vibration superimposed on the global mode shapes. The contribution of acoustic power radiated from these areas was calculated from

$$\Pi_v = \frac{\rho c}{E_r}\sum_{e=1}^{E_r} A_e v_{rms,e}^2$$

where A_e is the surface area of a face sheet element without any of the core attached, v_{rms} is the root-mean-square normal velocity and E_r is the total number of finite elements.

5   SOUND TRANSMISSION LOSS RESULTS

Mathematical computations were performed using Matlab[®] software. The random acoustic excitation fields were structured as matrix data files for input into the finite element bulk data deck. Velocity data from the finite element punch output files were assembled into matrices for the calculation of the radiation resistance matrix and the panel radiated power. The sound transmission loss was computed from the ratio of the radiated acoustic power and the power input for the panel excitation, and averaged over the ten random excitation fields. A finite element model of a 0.508 mm thick aluminum panel (same thickness and dimensions as one of the honeycomb face sheets) was generated to validate the sound transmission loss prediction method. The predictions were compared with the transmission loss of the same aluminum panel measured in the SALT[24] facility. The predicted and measured transmission loss data are shown in Figure 8. Good agreement, within 1.5 dB, was obtained between the predicted and measured data over the 300-1000 Hz frequency range. The disagreement was less than 5 dB for the frequencies below 300 Hz. The predicted and measured transmission loss data for the baseline honeycomb panel are compared in Figure 9. The trend of the data and the magnitude of the transmission loss were reasonably well predicted. Discrepancies between the predicted and measured curves were expected due to the uncertainties and tolerances in the finite element models, honeycomb material properties, boundary conditions and test procedures.
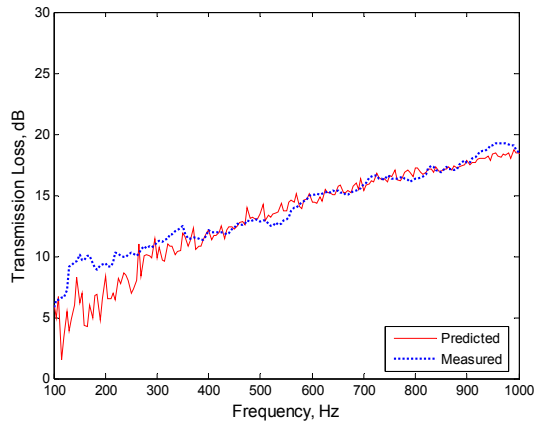

Figure 8. Predicted and measured sound transmission loss of a 0.51 mm thick aluminum panel.
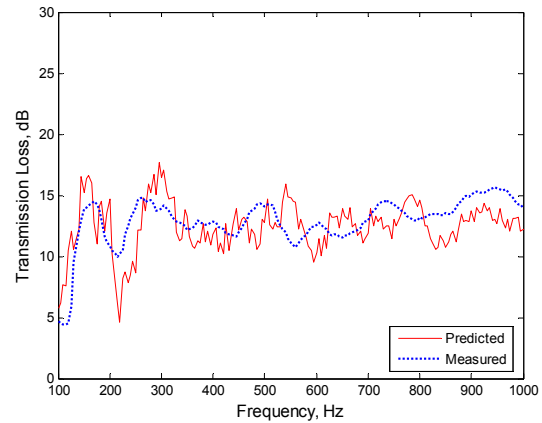

Figure 9. Predicted and measured sound transmission loss of the baseline honeycomb panel.

The finite element predicted sound transmission loss of the honeycomb panel with the nine 152 mm square voids (Voided 9-152) is in reasonable agreement with the measured data presented in Figure 10. The predicted improvement in transmission loss compared with the baseline panel is also confirmed by the measured transmission loss. Generally good agreement was obtained between the trends of the numerical predictions and the measured transmission loss for the Voided 9-254 panel in Figure 11. The larger voided areas, compared to the Voided 9-152 panel, resulted in higher predicted and measured transmission loss above 530 Hz. The mass-air-mass resonance due to the two face sheets on either side of the voids was calculated to occur at 525 Hz and was thought to be the cause for the dip in the transmission loss data (Figure 11). The third finite element model (Recessed 9-254) was designed to avoid this resonance and to reinforce the panel. The nine voided areas of this honeycomb panel were strengthened by leaving part of the core attached to the exterior face sheet and covering the exposed core in each area with a 0.41 mm thick aluminum patch. The cutout sections (Figure 7) of this configuration are
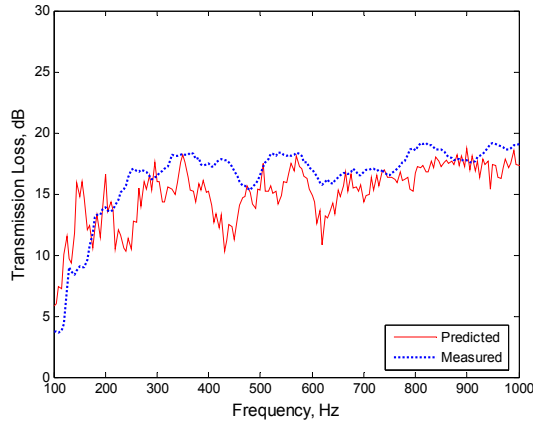
Figure 10. Predicted and measured sound transmission loss of a honeycomb panel featuring nine 152 mm square voids in the core (Voided 9-152).
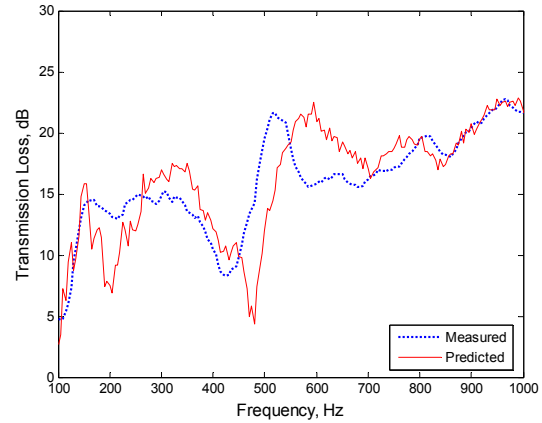

Figure 11. Predicted and measured sound transmission loss of a honeycomb panel featuring nine 254 mm square voids in the core (Voided 9-254).

bounded by the interior aluminum face sheet on one side and the 6.35 mm thick recessed core on the other side. The mass-air mass resonance is no longer visibly present in the predicted and measured transmission loss of Figure 12. Higher transmission loss was predicted for most of the frequency range above 160 Hz which was confirmed by the panel transmission loss measurements. It should be noted that the thickness of the recessed core of the test panel was 12.7 mm compared to a recessed core thickness of 6.35 mm for the panel in the predictions.
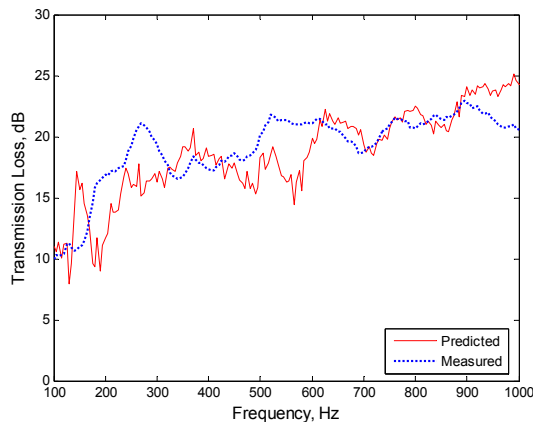

Figure 12. Predicted and measured sound transmission loss of a honeycomb panel featuring nine 254 mm patched, recessed core areas (Recessed 9-254).
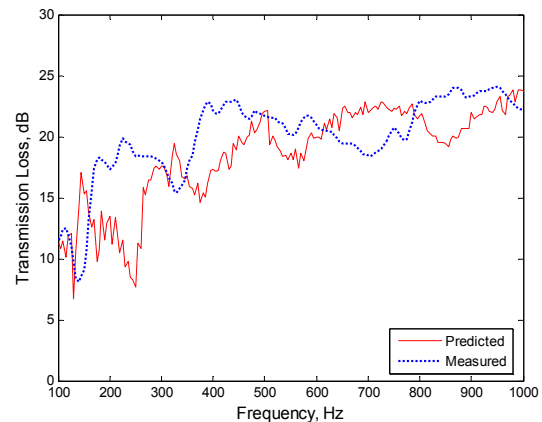

Figure 13. Predicted and measured sound transmission loss of a honeycomb panel featuring twenty-five 152 mm patched, recessed core areas (Recessed 25-152).

The fourth honeycomb panel configuration, designated Recessed 25-152, had about the same total recessed core area as the Recessed 9-254 panel (Table 2), but consisted of more areas with less separation area (Figure 14). The Recessed 25-152 panel had a slightly higher predicted and measured transmission loss than the Recessed 9-254 panel over most of the frequency region of interest (Figures 12 and 13). This fourth configuration improved the predicted transmission loss of the baseline panel by 2-11 dB in the frequency range from 320-1000 Hz. This was validated by the results of the transmission loss measured in the SALT facility where an improvement was observed from 3 to 11 dB over the frequency range 170-1000 Hz as shown in Figure 15. The mass of the Recessed 25-152 panel (5.78 kg) was only 5.1% more than the mass of the baseline
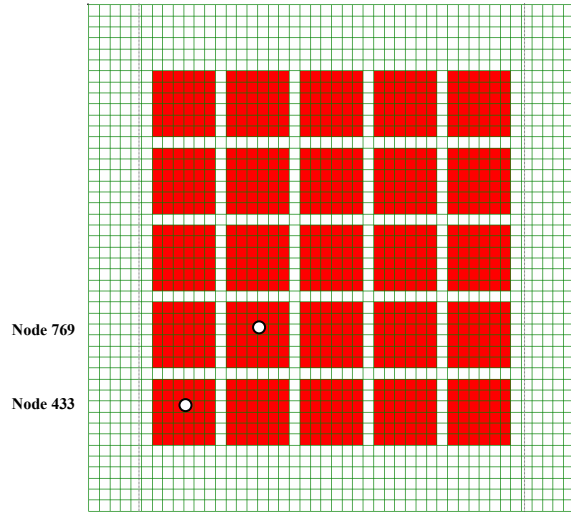
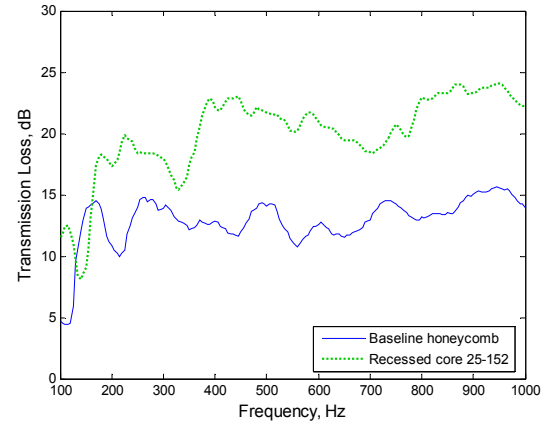Figure 14. Schematic for the locations of the twenty-five 152 mm by 152 mm voids in the honeycomb core.

Figure 15. Measured sound transmission loss of the baseline honeycomb panel and the panel featuring the twenty-five 152 mm patched, recessed core areas (Recessed 25-152).

honeycomb panel (5.50 kg). The stiffness of the baseline and the Recessed 25-152 honeycomb panels was numerically evaluated by applying a static 1 N point force at two different panel locations (Nodes 433 and 769 in Figure 14) on the exterior face sheet and computing the panel deflections using the finite element model. Measurements at those locations were also conducted to obtain the deflections for the same 1 N force on the honeycomb test panels. Table 3 shows that the panel deflections were predicted consistently higher (up to 25%) than the measured deflections. The deflection of the Recessed 25-152 panel was predicted and measured to have approximately twice the deflection of the baseline honeycomb panel at locations where the core was recessed from the radiating face sheet. Modal analyses are being planned to allow a more detailed explanation for the transmission loss curve behavior of the honeycomb panels.

Table 3. Displacement due to a unit static force at three node locations for two honeycomb panel configurations.

Panel configuration	Predicted deflection at node 769	Measured deflection at node 769	Predicted deflection at node 433	Measured deflection at node 433	Mass
	$[10^{-6}\,m]$	$[10^{-6}\,m]$	$[10^{-6}\,m]$	$[10^{-6}\,m]$	[kg]
Baseline honeycomb	3.0	2.89	2.0	1.72	5.4962
Recessed 25-152	6.0	5.38	4.0	3.20	5.7790

6   CONCLUDING REMARKS

Finite element models were developed of honeycomb panels featuring areas where the core was removed from the radiating face sheet disrupting the supersonic flexural and shear wave speeds that exist in the baseline panel. The sound radiation from these panels was reduced resulting in improved transmission loss for a defined diffuse sound field excitation. The models were verified with experimental results yielding reasonable agreement between the levels and trends in the transmission loss curves. The finite element models provided insight into the panel behavior leading to an optimized design configuration with a transmission loss improvement of 3-11 dB compared to the baseline honeycomb panel over a frequency range from 170-1000 Hz. The improved transmission loss panel configuration had a 5.1% increase in mass and twice the deflection of the baseline honeycomb panel when excited by a static force.

7   ACKNOWLEDGEMENTS

8   REFERENCES

[1]   Grosveld, F. W. and Mixson, J. S., "Noise Transmission through an Acoustically Treated and Honeycomb Stiffened Aircraft Sidewall," J. Aircraft, **22** (5), May 1985, pp. 434-441.

[2]   Kurtze, G. and Watters, B. G., "New Wall Design for High Transmission Loss or High Damping," J. Acoust. Soc. Am. **31** (6), 739–748, 1959.

[3]   Davis, Evan. B., "Designing Honeycomb Panels for Noise Control," AIAA-99-1917.

[4]   Wen-chao, Huang and Chung-fai, Ng., "Sound Insulation Improvement using Honeycomb Sandwich Panels," Applied Acoustics, Vol. 53, No. 1-3, pp. 163-177, 1998.

[5]   Clarkson, L. and Ranky, M. F., "Modal Density of Honeycomb Plates," J. Sound Vib. **91**, 103–118, 1983.

[6]   Renji, K., Nair, P. S. and Narayanan, S., "Modal Density of Composite Honeycomb Sandwich Panels," J. Sound Vib. **195** (5), 687–699, 1996.

[7]   Nilsson E. and Nilsson, A. C., "Prediction and Measurement of Some Dynamic Properties of Sandwich Structures with Honeycomb and Foam Cores," J. Sound Vib. **251** (3), 409–430, 2002.

[8]   Meraghni, F., Desrumaux, F. and Benzeggagh, M. L., Mechanical Behaviour of Cellular Core for Structural Sandwich Panels," Composites: Part A 30 (1999), pp. 767-779.

[9]   Nilsson E., "Some Acoustic and Dynamic Properties of Honeycomb Panels," AIAA-98-2344, 1998.

[10]   He, Hua and Gmerek, Mark, "Measurement and Prediction of Wave Speeds of Honeycomb Structures," AIAA-99-1965, 1999.

[11]   Mathur, G., Gardner, B., Phillips, J. and Burge, P., "An Experimental Technique of Separating Air Borne and Structure Borne Noise Using Wavenumber-Frequency Spectrum," AIAA-90-3969, 1990.

[12]   Mathur, G. and Tran, B., "Wavenumber Active Structural Acoustic Control for Smart Structures," AIAA-93-4422, 1993.

[13]   Williams, Earl, G. "Supersonic Acoustic Intensity on Planar Sources," J. Acoust. Soc. Am. **104** (5), November 1998.

[14]   Jiang, L., Liew, K. M., Lim, M. K. and Low, S. C., "Vibratory Behaviour of Delaminated Honeycomb Structures: A 3-D Finite Element Modeling," Computers and Structures, Vol. 55, No. 5, pp. 773-788, 1995.

[15]   Grediac, M., "A Finite Element Study of the Traverse Shear in Honeycomb Cores," Int. J. Solids Structures, Vol. 30, No. 13, pp. 1777-1788, 1993.

[16]   Xu, X. Frank and Qiao, Pizhong, "Homogenized Elastic Properties of Honeycomb Sandwich with Skin Effect," Int. J. Solids and Structures, **39**, pp. 2153-2188, 2002.

[17]   Ghinet, Sebastian, Atalla, Noureddine and Osman, Haisam, "The Transmission Loss of Curved Laminates and Sandwich Composite Panels," J. Acoust. Soc. Am. **118** (2), August 2005.

[18]   Buehrle, Ralph D., Robinson, Jay H. and Grosveld, Ferdinand W., "Vibroacoustic Model Validation for a Curved Honeycomb Composite Panel," AIAA-2001-1587, 2001.

[19]   Grosveld, Ferdinand W., Buehrle, Ralph D. and Robinson, Jay H., "Structural and Acoustic Modeling of a Curved Composite Honeycomb Panel," AIAA-2001-2277, 2001.

[20]   Buehrle, Ralph D., Klos, Jacob, Robinson, Jay H. and Grosveld, Ferdinand W., "Structural Acoustic Modeling of Aircraft Fuselage Structures," First Pan-American//Iberian Meeting on Acoustics, 144th Meeting of the Acoustical Society of America, 2-6 December 2002.

[21]   Barisciano, Lawrence, P., "Broadband transmission Loss Due to Reverberant Excitation," NASA Contractor Report NASA-99-CR209687, 1999.

[22]   Klos, J., Robinson, J. H., and Buehrle, R. D., "Sound Transmission Through a Curved Honeycomb Composite Panel," AIAA-2003-3157, 2003.

[23]   Robinson, J. H., Buehrle, R. D., Klos, J. and Grosveld, F. W., "Radiated Sound Power from a Curved Honeycomb Panel," AIAA 2003-3156, 2003.

[24]   Grosveld, Ferdinand W., "Calibration of the Structural Acoustic Loads and Transmission (SALT) facility at NASA Langley Research Center," INTER-NOISE 99 International Congress on Noise Control Engineering, Fort Lauderdale, Florida, December 6-8, 1999.

[25]   Kinsler, L. E. and Frey, A. R, *Fundamentals of Acoustics*, 2nd ed., Wiley 1962.

[26]   Elliott S. J. and Johnson, M. E., "Radiation Modes and the Active Control of Sound Power," J. Acoust. Soc. Am. **94** (2), August 2005.

FINITE ELEMENT DEVELOPMENT OF
HONEYCOMB PANEL CONFIGURATIONS
WITH IMPROVED SOUND TRANSMISSION LOSS

Ferdinand W. Grosveld
Lockheed Martin Engineering and Sciences

Daniel L. Palumbo, Jake Klos and **William D. Castle**
NASA Langley Research Center

Mailing address:	NASA Langley Research Center	*Electronic Mail:*
	Mail Stop 463	f.w.grosveld@larc.nasa.gov
	Hampton, VA 23681	*Facsimile:*
	(757) 864-3586	(757) 864-4449

INTRODUCTION

Sandwich type panels, where a honeycomb core is sandwiched between two facesheets, has found widespread use in the aerospace industry as aircraft floor and wall panels. The higher stiffness-to-mass ratio of a honeycomb panel compared to a homogeneous panel results in a lower acoustic critical frequency. At the critical frequency a resonance occurs when the structural flexural wavelength matches the wavelength of the incoming sound. Above the critical frequency resonances occur at different angles of sound incidence as the sound trace wavelength equals the structural bending wavelength. The flexural wave speed is called supersonic at these coincidence frequencies and the structure becomes a very efficient radiator over its entire surface resulting in a lower sound transmission loss than exhibited by a homogeneous panel of the same mass.[1] Researchers have tried to improve the transmission loss performance by optimizing the mechanical properties of the panels or by increasing the structural damping.[2-4] Modal distribution,[5,6] dynamic properties,[7-9] and acoustic characteristics[9] of honeycomb panels have been investigated to obtain a better understanding of the vibro-acoustic response of these sandwich structures. The wavenumber frequency spectrum has been employed to illustrate the dispersion behavior of a panel below and above the critical frequency.[11-13] The vibratory behavior of the honeycomb panel has been numerically modeled in numerous publications, some of which[14-17] are listed in the References section. Non-resonant and resonant transmission loss of sandwich structures were computed in Reference 15 with the use of dispersion curves, panel radiation efficiency and panel modal density. Structural-acoustic finite element and boundary element models have recently been developed at the NASA Langley Research Center to describe and predict the sound radiation from and the transmission loss of honeycomb type structures.[18-23] In the proposed paper finite element models are presented of honeycomb structures that feature voids in their honeycomb cores to disrupt the supersonic flexural wave speed that exists in the baseline honeycomb panel. It will be shown that the sound radiation from these 'voided' honeycomb panels can be constrained resulting in lower acoustic emission and improved sound transmission loss. The models were verified with the experimental sound radiation and transmission loss results from honeycomb panels in the Structural Acoustic Loads and Transmission (SALT) facility at NASA Langley. The frequency of interest for the finite element models was limited to a narrowband analysis (5 Hz bandwidth) up to 1000 Hz.

FINITE ELEMENT MODELING

Finite element models were developed using the pre/post processor MSC/PATRAN 2005 and were analyzed with different solution methods in MSC/NASTRAN 2005. Modal analyses were performed to obtain the modal characteristics of the honeycomb panels. Frequency response functions were computed for excitation by ten sets of random amplitude and random angle of incidence sound fields. Velocity distributions over the panel surface were output in NASTRAN punch files for post processing.

MATLAB COMPUTATIONS

Mathematical computations were performed in MATLAB software to compose the random acoustic excitation fields, obtain the acoustic pressures from the panel velocity distribution and to propagate the resulting pressures into the acoustic far field. The sound transmission loss was computed and averaged for the ten excitation fields.

SOUND TRANSMISSION LOSS RESULTS

A finite element model of a 0.508 mm thick aluminum panel (same thickness as one of the honeycomb facesheets) was generated to validate the sound transmission loss (TL) prediction method. The TL predictions were compared with the measured TL of an aluminum panel with the same thickness and a sound exposed area of 1.15 m by 1.15 m. The TL experiments were conducted in the SALT[24] facility. The predicted and measured TL data are shown in Figure 1 and were within 1 dB agreement for the 300 Hz – 1000 Hz frequency range. A discrepancy of less than 4 dB was achieved for frequencies below 300 Hz. The base honeycomb panel consisted of a 19.05 mm thick Nomex core, sandwiched between two 0.508 mm thick aluminum facesheets. The mechanical properties of the honeycomb panels will be described in detail in the proposed paper. The measured and predicted TL of the baseline honeycomb panel (designated SNC) showed good agreement as evidenced in Figure 2. The improved honeycomb model featured nine 0.1524 m by 0.1524 m voids in the honeycomb core material. The voids were distributed over the core as illustrated in Figure 3. Generally good agreement was obtained between the numerical predictions and the measured sound transmission loss as depicted in Figure 4. Figure 5 shows the configuration of the honeycomb panel with nine 0.254 m by 0.254 m voids in the core material. The experimental TL of this configuration is compared with the experimental results of the honeycomb panel with the nine 0.1524 m by 0.1524 m voids in Figure 6. Several other 'voided' honeycomb panels, with different void sizes and void distributions, were tested and compared with the predictions from the finite element models. New honeycomb panel configurations were designed to further improve sound transmission loss. The panel designs had the same square area cut out of the core but through only part of the core thickness, leaving some of the honeycomb core attached to one of the facesheets to preserve part of the panel stiffness. The proposed paper will present the results for several honeycomb panel configurations for which the cutout area, thickness, and distribution were varied. Results of several parameter studies of the mechanical and material properties will be discussed.

REFERENCES

1. Grosveld, F. W. and Mixson, J. S., "Noise Transmission through an Acoustically Treated and Honeycomb Stiffened Aircraft Sidewall," Journal of Aircraft, Vol. 22, No. 5, May 1985, pp. 434-441.

2. Kurtze, G. and Watters, B. G., "New Wall Design for High Transmission Loss or High Damping," J. Acoust. Soc. Am. 31 6, 739–748, 1959.

3. Davis, Evan. B., "Designing Honeycomb Panels for Noise Control," AIAA-99-1917.

4. Wen-chao, Huang and Chung-fai, Ng., "Sound Insulation Improvement using Honeycomb Sandwich Panels," Applied Acoustics, Vol. 53, No. 1-3, pp. 163-177, 1998.

5. Clarkson, L. and Ranky, M. F., "Modal Density of Honeycomb Plates," J. Sound Vib. 91, 103–118, 1983.

6. Renji, K., Nair, P. S. and Narayanan, S., "Modal Density of Composite Honeycomb Sandwich Panels," J. Sound Vib. 195 5, 687–699, 1996.

7. Nilsson E. and Nilsson, A. C., "Prediction and Measurement of Some Dynamic Properties of Sandwich Structures with Honeycomb and Foam Cores," J. Sound Vib. 251 3, 409–430, 2002.

8. Meraghni, F., Desrumaux, F. and Benzeggagh, M. L., Mechanical Behaviour of Cellular Core for Structural Sandwich Panels," Composites: Part A 30 (1999), pp. 767-779.

9. Nilsson E., "Some Acoustic and Dynamic Properties of Honeycomb Panels," AIAA-98-2344.

10. He, Hua and Gmerek, Mark, "Measurement and Prediction of Wave Speeds of Honeycomb Structures," AIAA-99-1965.

11. Mathur, G., Gardner, B., Phillips, J. and Burge, P., "An Experimental Technique of Separating Air Borne and Structure Borne Noise Using Wavenumber-Frequency Spectrum," AIAA-90-3969, 13th AIAA Aeroacoustics Conference, Tallahassee, Florida, 22-24 October 1990.

12. Mathur, G. and Tran, B., "Wavenumber Active Structural Acoustic Control for Smart Structures," AIAA-93-4422, 15th AIAA Aeroacoustics Conference, Long Beach, CA, 25-27 October 1993.

13. Williams, Earl, G. "Supersonic Acoustic Intensity on Planar Sources," J. Acoust. Soc. Am. 104 5, November 1998.

14. Jiang, L., Liew, K. M., Lim, M. K. and Low, S. C., "Vibratory Behaviour of Delaminated Honeycomb Structures: A 3-D Finite Element Modeling," Computers and Structures, Vol. 55, No. 5, pp. 773-788, 1995.

15. Grediac, M., "A Finite Element Study of the Traverse Shear in Honeycomb Cores," Int. J. Solids Structures, Vol. 30, No. 13, pp. 1777-1788, 1993.

16. Xu, X. Frank and Qiao, Pizhong, "Homogenized Elastic Properties of Honeycomb Sandwich with Skin Effect," Int. J. Solids and Structures, 39, pp. 2153-2188, 2002.

17. Ghinet, Sebastian, Atalla, Noureddine and Osman, Haisam, "The Transmission Loss of Curved Laminates and Sandwich Composite Panels," J. Acoust. Soc. Am. 118 2, August 2005.

18. Buehrle, Ralph D., Robinson, Jay H. and Grosveld, Ferdinand W., "Vibroacoustic Model Validation for a Curved Honeycomb Composite Panel," AIAA-2001-1587, 42nd AIAA/ASME/ASCE/AHS/ASC Structures, Structural Dynamics, and Materials Conference, Seattle, Washington, 16-19 April 2001, pp. 9.

19. Grosveld, Ferdinand W., Buehrle, Ralph D. and Robinson, Jay H., "Structural and Acoustic Modeling of a Curved Composite Honeycomb Panel," AIAA-2001-2277, 7th AIAA/CEAS Aeroacoustics Conference, Maastricht, The Netherlands, 28-30 May 2001, pp. 11.

20. Buehrle, Ralph D., Klos, Jacob, Robinson, Jay H. and Grosveld, Ferdinand W., "Structural Acoustic Modeling of Aircraft Fuselage Structures," First Pan-American//Iberian Meeting on Acoustics, 144th Meeting of the Acoustical Society of America, 3rd Iberoamerican Congress of Acoustics, 9th Mexican Congress of Acoustics, Fiesta Americana Grand Coral Beach Hotel in Cancun, Mexico, 2-6 December 2002.

21. Barisciano, Lawrence, P., "Broadband transmission Loss Due to Reverberant Excitation," NASA Contractor Report NASA-99-CR209687, 1999.

22. Klos, J., Robinson, J. H., Buehrle, R. D., "Sound Transmission Through a Curved Honeycomb Composite Panel," AIAA-2003-3157, 9th AIAA/CEAS Aeroacoustics Conference and Exhibit, Hilton Head, South Carolina, 12-14 May 2003.

23. Robinson, J. H., Buehrle, R. D., Klos, J. and Grosveld, F. W., "Radiated Sound Power from a Curved Honeycomb Panel," AIAA Paper 2003-3156, presented at the 9th AIAA/CEAS Aeroacoustics Conference and Exhibition, Hilton Head, South Carolina, 12-14 May 2003.

24. Grosveld, Ferdinand W., "Calibration of the Structural Acoustic Loads and Transmission (SALT) facility at NASA Langley Research Center," presented at the INTER-NOISE 99 International Congress on Noise Control Engineering, Fort Lauderdale, Florida, December 6-8, 1999.
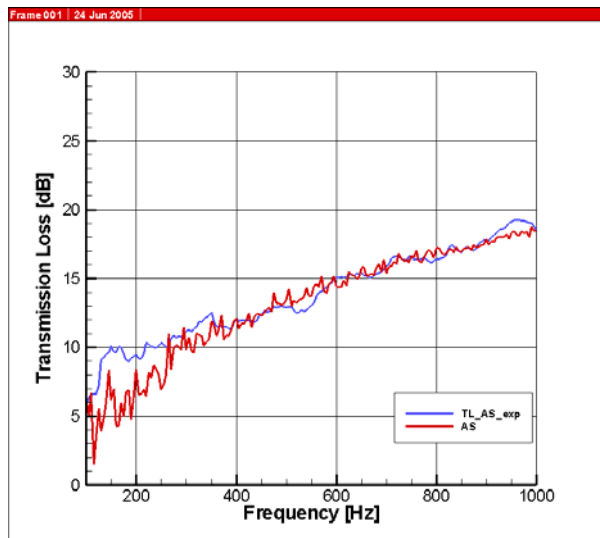
FIGURES

Figure 1. Measured (TL_AS_exp) and predicted (AS) sound transmission loss (TL) of a 0.508 mm thick aluminum panel.
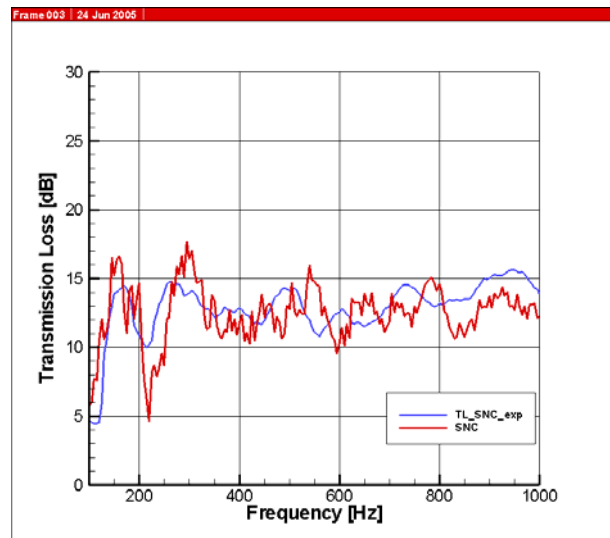
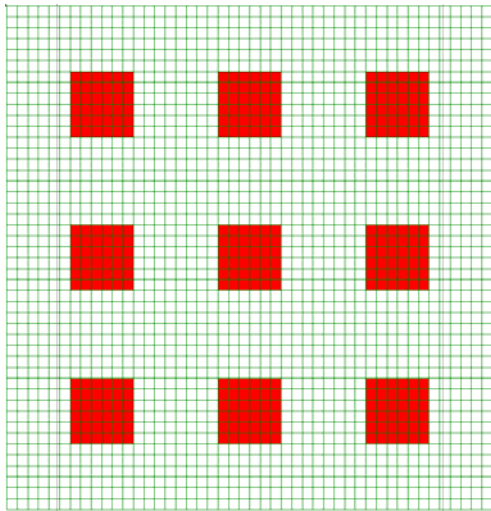Figure 2. Measured (TL_SNC_exp) and predicted (SNC) sound transmission loss of the baseline honeycomb panel.

Figure 3. Schematic of the 46 by 46 elements finite element model and the locations of the nine 0.1524 m by 0.1524 m voids in the honeycomb core material.
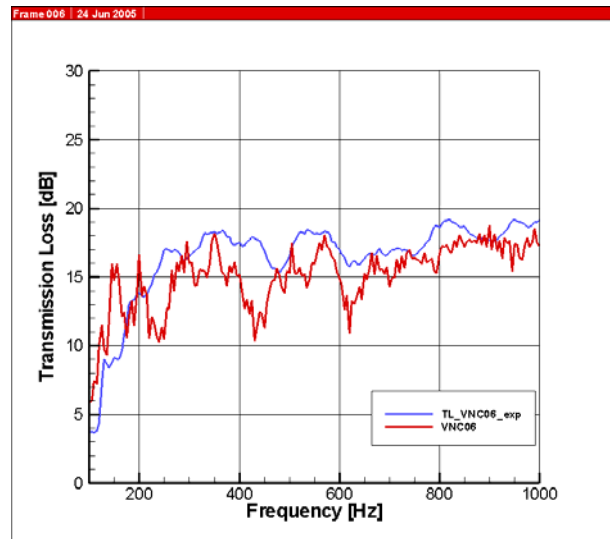

Figure 4. Measured (TL_VNC06_exp) and predicted (VNC06) sound transmission loss of the 'voided' honeycomb panel.
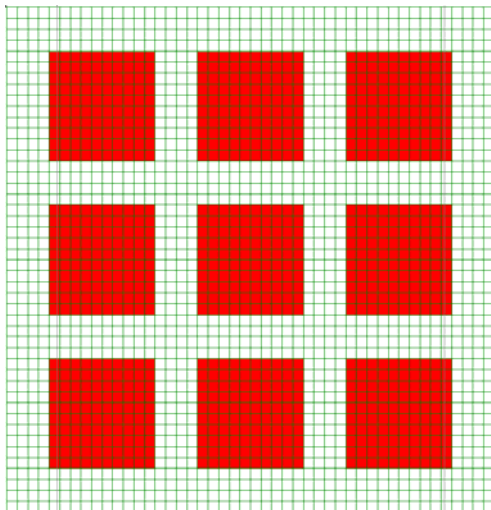

Figure 5. Schematic of the honeycomb panel finite element model showing the locations of the nine 0.254 m by 0.254 m voids in the core.
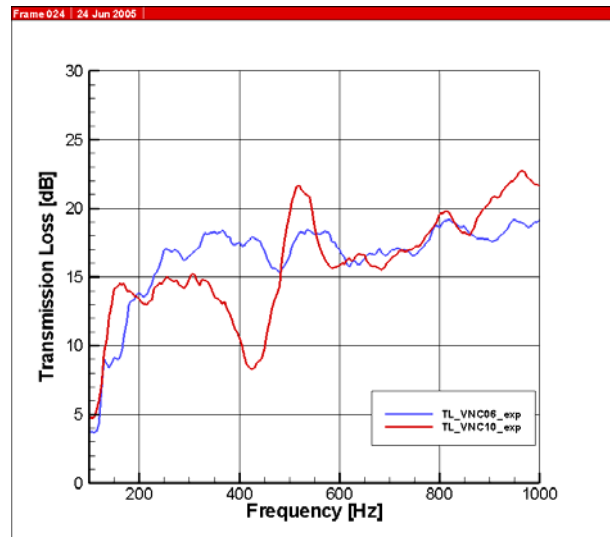

Figure 6. Measured TL of honeycomb core panels with nine 0.1524 m by 0.1524 m (TL_VNC06_exp) and nine 0.254 m by 0.254 m voids (TL_VNC10_exp).